

Numerical Simulation of Air Flow Field of A Gas Turbine Engine Air blast Atomizer

Syed Habeebur Rahaman^{1*}, P.N. Tengli², Rampada Rana³, Srikanth H.V.⁴

Abstract

One of the most crucial process that occurs before the fuel is burned in the combustion chamber is atomization. The performance of a engine will be depend mainly on the fuel mixture. Performance of the engine depends on atomization process because it breaks the bulk fuel into small droplets and injects it into the combustion chamber, in order to make this happen consequently the dimensions of most of the fuel droplets ought to have Sauter Mean Diameter/Same Diameter (SMD) in order that the time for combustion of each fuel droplet remains same. The air blast atomizer uses the kinetic energy of a flowing airstream to disintegrate fuel into ligaments and then into small droplets. Since numerical simulation of the atomizer is complex it is very important to understand the air flow, which is used for fuel atomization in air blast atomizer. CFD analysis at atmospheric conditions was performed in this paper using ANSYS Fluent to validate modelling methodology from accuracy and reliability point of view. The following analysis involves the studies of downstream domain parametrically and selection of the final downstream domain which conforms to the physics of the flow field which have been discussed in detail. Studies on the opted downstream domain were further continued using various air mass flows. Plots were drawn for axial, radial, and tangential velocities, as well as the recirculation zone. Because the flow field in atmospheric settings may be utilized to investigate droplets tracking to compare the test performance data at atmospheric conditions, this research aids in understanding the type of downstream domain needed for atmospheric conditions.

Keywords: Gas turbine, Air blast atomizer, Air flow field, Re-circulation zone, Velocity Plots.

INTRODUCTION

In order to atomize a liquid, it is frequently injected into a stream of gas or air that is flowing relatively slowly. One of the first to investigate the theoretical breakdown of liquid jets was Rayleigh [1]. He commenced by taking the simple situation of a laminar jet emerging from a circular orifice and postulated a breakup process. The distinct kinds of atomizers such as pressure and rotary atomizers, which expel liquid at a greater velocity from the edge of a revolving disc, are notable examples. An alternative approach is to subject a relatively slow moving liquid to a greater velocity air flow. The latest method is commonly known as twin fluid atomization, air assist or air blast. The fuel injection process, which affects many aspects of combustion performance, will likely become even more crucial as regulations for pollutant emissions become more rigorous and all types of incinerators are forced to burn fuels of decreasing quality. Reduced mean fuel droplet size results in higher volumetric heat release rates, easier ignition, a wider combustion

*Author for Correspondence

Syed Habeebur Rahaman

¹PG Student, Department of Aeronautical Engineering, Nitte Meenakshi Institute of Technology, Bangalore, Karnataka, India

²Professor, Department of Aeronautical Engineering, Nitte Meenakshi Institute of Technology, Bangalore, Karnataka, India

³Scientist E, Gas Turbine Research Establishment, Bangalore, Karnataka, India

⁴Associate Professor, Department of Aeronautical Engineering, Nitte Meenakshi Institute of Technology, Bangalore, Karnataka, India

Received Date: November 04, 2023

Accepted Date: January 05, 2024

Published Date: March 08, 2024

Citation: Syed Habeebur Rahaman, P.N. Tengli, Rampada Rana, Srikanth H.V. Numerical Simulation of Air Flow Field of A Gas Turbine Engine Air blast Atomizer. Journal of Polymer & Composites. 2023; 11(Special Issue 13): S169–S180.

range, and lower pollutant concentrations in most combustion systems [2, 3, 4]. Atomizers must have a best atomization process over different flow rates (turndown ratio), be free of flow instabilities, and be low cost, light weight, easy to maintain, and disassemble for service [5]. After achieving higher specific fuel burn and higher specific thrust of the gas turbine engine, it has already been established that the gas turbine characteristics meeting the demands for better combustion performance in terms of combustion efficiency, flame stability, better ignition characteristics, and lower emissions, etc. [6]. Hinze [7] employed a dimensionless group known as the Ohnesorge number to take the effect of liquid viscosity on droplet breakage into account. According to Rana et al. [8], a better injector near the flow field achieves smaller droplet sizes and better mass atomization of the fuel into droplets, as well as droplet distribution through terms of smaller droplet sizes and uniform velocities. When a consistent mixture of fuel vapour and air is burned at a low temperature, NO_x emissions from the combustion chamber can be controlled. Consequently, the injector is essential for achieving higher combustion performance [9]. In a realistic combustor, Sankaran and Menon [10] used LES to capture the unstable interaction between spray dispersion, evaporation, fuel-air mixture, and heat release. They found that the presence of high eddy is the main factor that increased droplet dispersion and activated CTRZ. The aerospace industry and academia are increasingly interested in combustion research involving alternative fuels because of the advantages they provide, including better air quality, a more diverse fuel supply, and affordable fuel sources [11].

Pressure vortex atomizers, air blast atomizers, or a combination of both are frequently used in gas turbine combustion applications to atomize the fuel [12]. The air blast atomizer is the most popular. On an air blast atomizer, Rizkalla and Lefebvre conducted parametric tests to examine the impact of various physical characteristics on aerosols produced under various operating situations [13, 14]. A research on the effects of fuel temperature on atomization for various pressure swirl atomizers was done by Wang and Lefebvre [15]. Throughout the trial, the fuel injection pressure was changed, and it was noticed that as the pressure grew, the size of the droplets shrank. Giffen and Muraszew [16] claim that According to research, increasing air viscosity, surface tension, and temperature led to larger droplet sizes and less effective atomization. According to recent research by Zheng et al. [17,18], the air/fuel drive ratio is the main factor controlling the angle of the spray cone in a counter-rotating air jet atomizer running kerosene fuel. The circumferential pattern of aerosols produced by pressure vortex nebulizers is seldom ever discussed in the literature. To investigate the effects of differences in fluid characteristics, operating circumstances, and atomizer design elements on the spray pattern. According to the authors' understanding, none of the aforementioned studies involved the combustion chamber's upstream domain (the airbox) and a variety of downstream domains that were arbitrarily chosen based on their size and other factors [19, 20].

The choice of the downstream domain and the analysis is conducted by plotting various velocity plots at various downstream sites. Plotting axial, radial, and tangential velocities at two different downstream domain locations along with the recirculation zone resulted in the configuration and analysis of three downstream domains. The domain with the least difference was chosen as the best domain, and grid independent study was carried out further on the selected domain. The simulation results and experimental data were compared for this domain thus validating the modelling methodology.

COMPUTATIONAL METHODOLOGY

In the field of computational fluid dynamics, heat transfer and fluid flow-related issues are solved and analyzed using numerical methods and data structures. By taking into account the equations for the conservation of mass, momentum, and energy the Navier-Stokes equations are solved to model the fluid flow and heat transfer problem [10].

Geometry details

From Figure 1 there is an inlet (1) for the flow of fluid (air) followed by air box (2) wherein the air blast atomizer (Figure 2) is placed for testing purpose, then it comes the downstream domain (3) which

has converging section just before the outlet (4). The dimensions of the model is shown in Table 1. The geometry has been modelled in CAD software for the numerical analysis, and the fluid extraction and geometry cleaning have been finished in Space Claim. At the downstream, three additional domains are introduced in accordance with the simulation requirements.

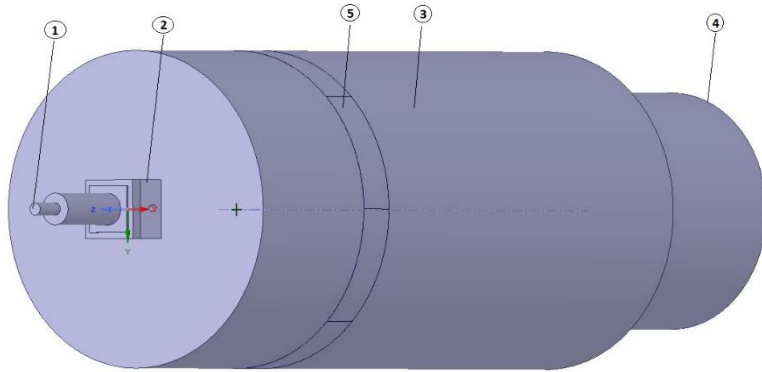


Figure 1. First domain.

Table 1. Dimensions of the first model

S.N.	Part	Dimensions (mm)
1.	Inlet Diameter	30.55
2.	Downstream Diameter	778
3.	Outlet Diameter	579

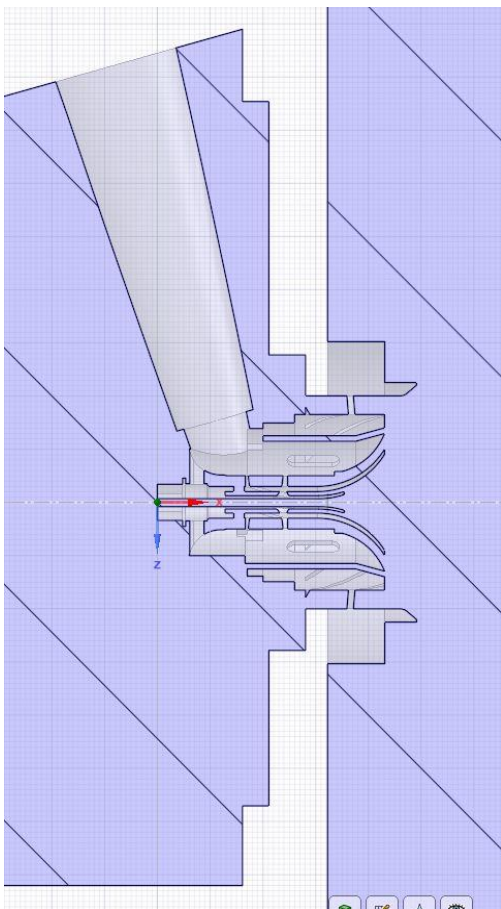


Figure 2. Inside the atomizer.

Grid details, Domain Selection, Numerical Studies

The accuracy and correctness of the CFD analysis relies upon the quality of the mesh and CFD evaluation of a complicated part is essential. The observations of various researchers [21] have highlighted the need for more information on how and to what extent distributions and liquid volumes are affected by the nozzle. Design features, nozzle dimensions, eccentric alignment of key nozzle components, surface defects, fluid properties, and nozzle operating conditions. The atomizer is a complex part as it consists of various individual components that have different dimensions and cross-sections and are assembled to form the atomizer. Therefore, care was taken to assign the grid size with different type of meshes to various parts within the air blast atomizer (Figure 3) (Table 2).

The simulations were carried out using three different downstream domains with wall boundary and pressure far field conditions leading to a total 5 test cases.

For the first downstream domain diameter of the outlet and the downstream being 579 mm and 778 mm respectively.

For the second (Doubled) domain diameter of the outlet and the downstream being doubled, i.e. 1158 mm and 1556 mm respectively and for the third domain (Enlarged refinement zone), the refinement zone was doubled with the reference to the first and second downstream domains.

Plots of X/d vs u/V_b , were X/d is the distance along x-axis and u/V_b , v/V_b and w/V_b are axial velocity (u), radial velocity (v) and tangential velocity (w) in y-axis respectively were plotted at two different locations along with re-circulation zone for three different downstream domains with two different boundary conditions so that the variation of results can be compared and subsequently the best downstream could be chosen (Figure 4).

Observation: In the first domain with the wall condition, which is what creates the flow symmetry in the downstream domain, there is no wall effect, as can be seen in Figure 5. In contrast, the flow is asymmetric in other domains with a different boundary condition because of the influence of the wall condition.

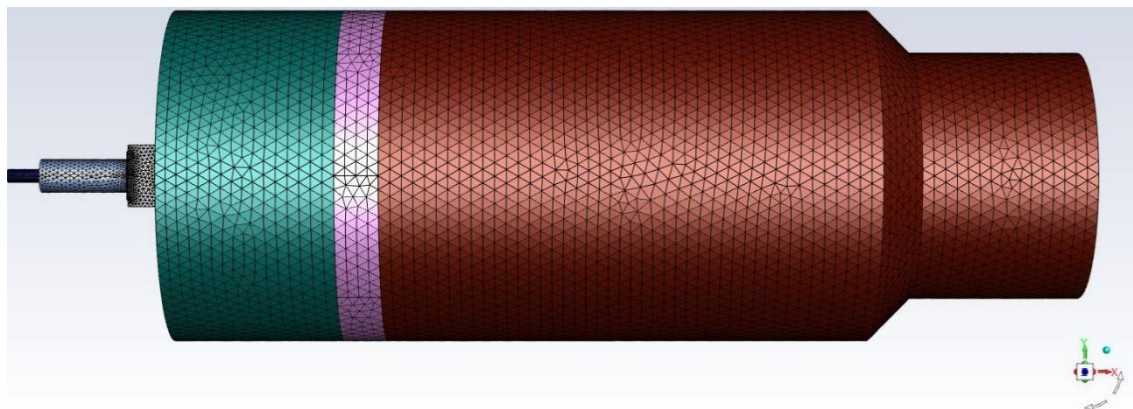


Figure 3. View of first domain with surface mesh.

Table 2. Quality check for three domains.

S.N.	Quality Check	First/Original domain	Second/Doubled downstream domain	Third/Enlarged refinement zone domain
1.	Aspect ratio	25.5	24.7	26.8
2.	Orthogonality	0.1	0.1	0.1
3.	Skewness	0.8	0.8	0.8
4.	Cell count (Million)	6.8	4.8	9.8

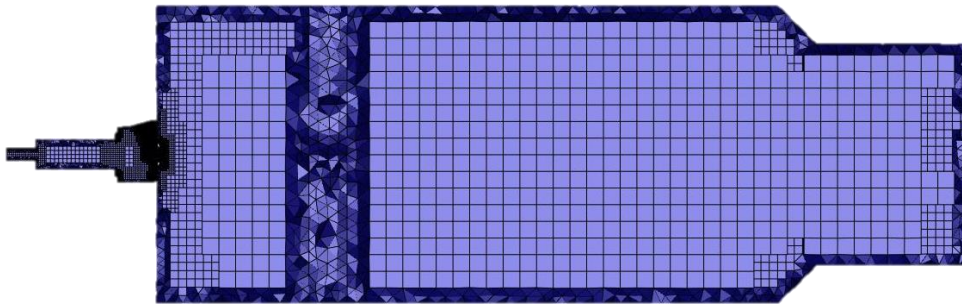


Figure 4. View of first domain with volume mesh.

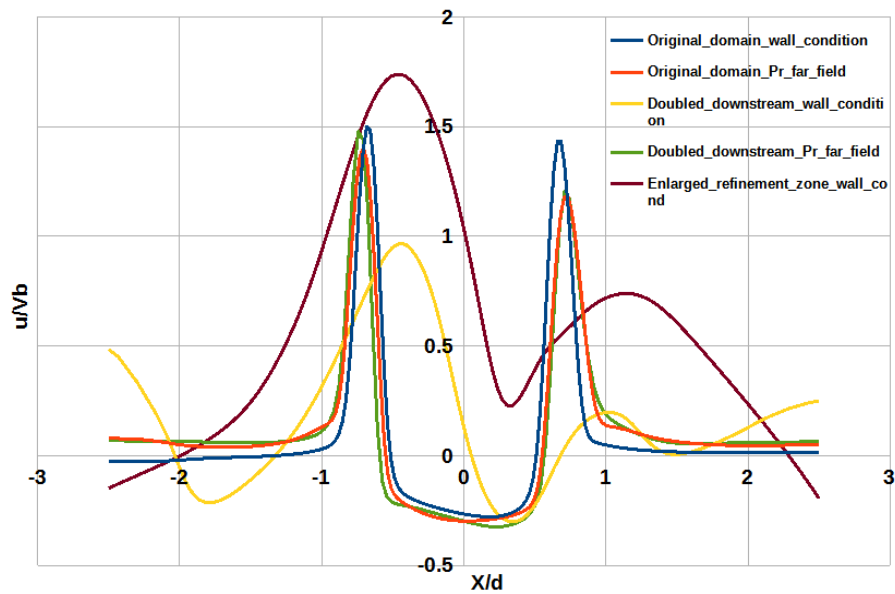


Figure 5. Distribution of axial velocity at $X/d=1.5$ across different domains and B.C.

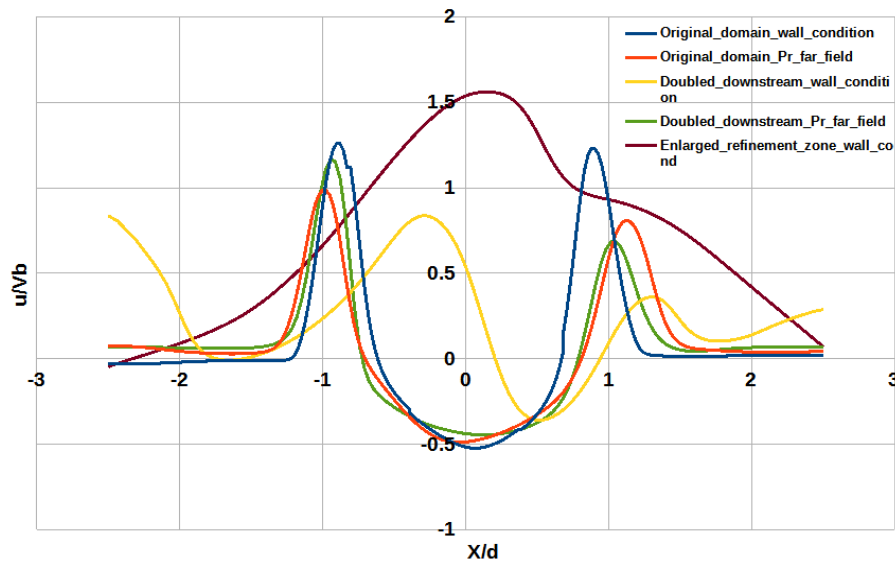


Figure 6. Distribution of axial velocity at $X/d=1.8$ across different domain and B.C.

Observation: Figure 6 shows that the wall condition in the first domain with the symmetric flow in the downstream domain has no wall impact. In contrast, the flow is asymmetric in other domains with a different boundary condition because of the influence of the wall condition.

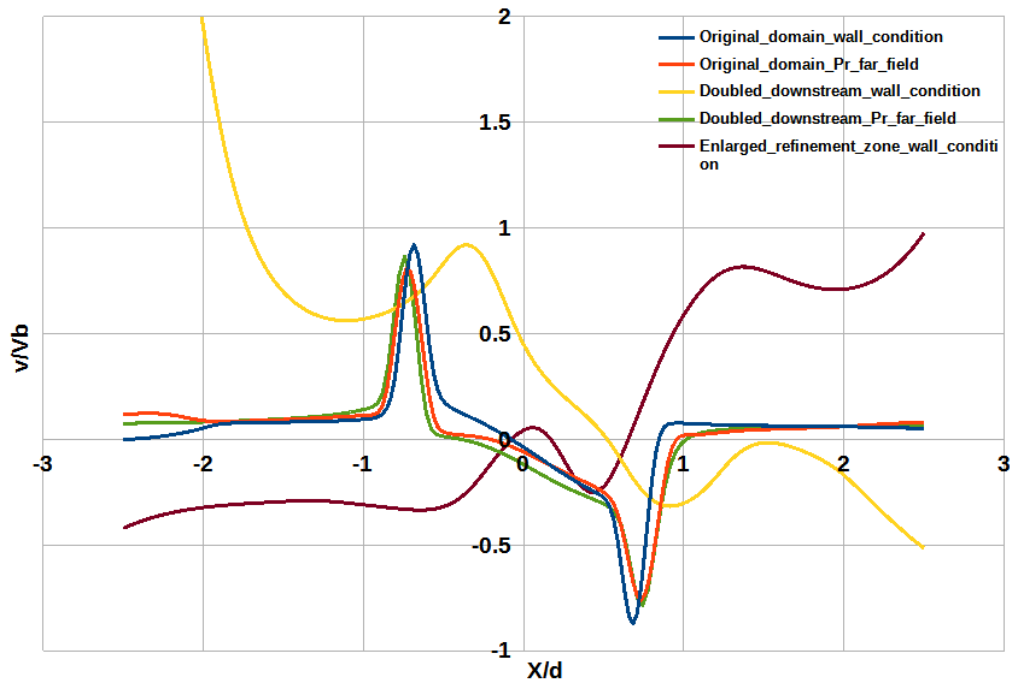


Figure 7. Distribution of radial velocity at $X/d=1.5$ across different domain and B.C.

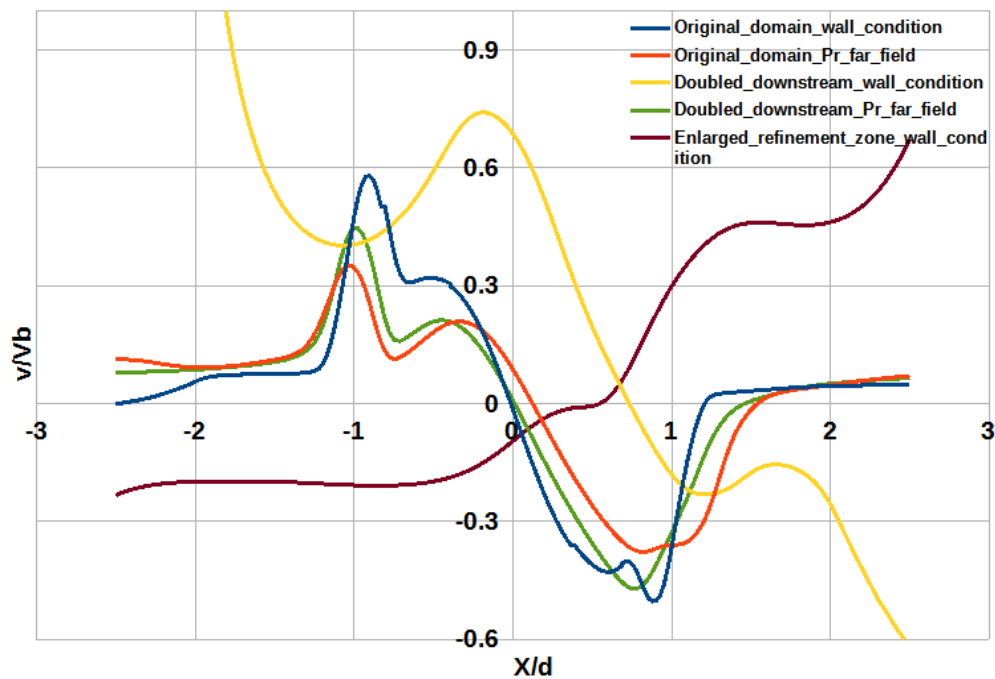


Figure 8. Distribution of radial velocity at $X/d=1.8$ across different domain and B.C.

Observation: In the first domain with the wall condition, which is what creates the flow symmetry in the downstream domain, there is no wall effect, as can be seen in Figure 7. In contrast, the flow is asymmetric in other domains with a different boundary condition because of the influence of the wall condition.

Observation: Figure 8 shows that there is no wall effect in the first domain with a wall condition, resulting in the downstream domain's flow symmetry. In contrast, the flow is asymmetric in other domains with a different boundary condition because of the influence of the wall condition.

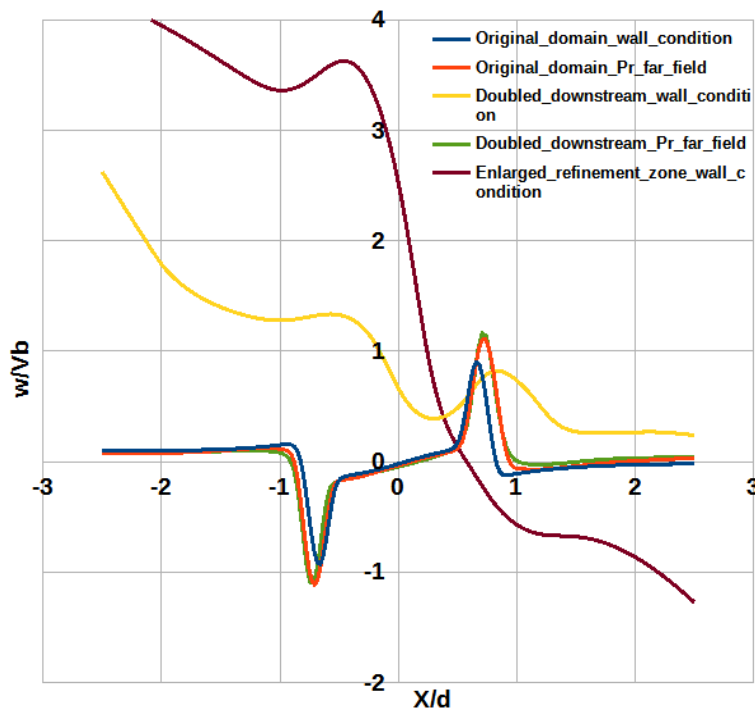


Figure 9. Distribution of tangential velocity at $X/d=1.5$ across different domain and B.C.

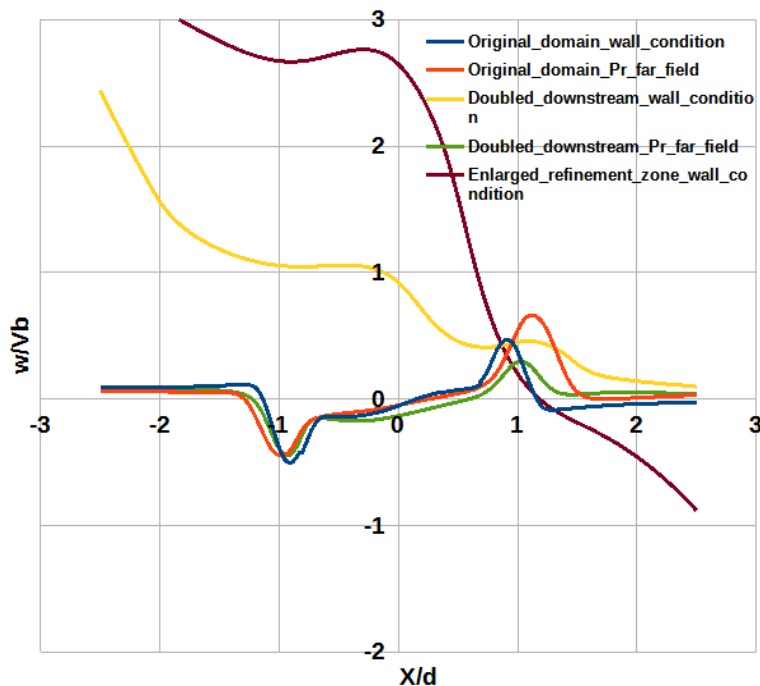


Figure 10. Distribution of tangential velocity at $X/d=1.8$ across different domain and B.C.

Observation: Figure 9 shows that there is no wall effect in the first domain with the wall condition, resulting in flow symmetry in the downstream domain. In other domains with different boundary conditions, the flow is asymmetric due to the effect of the wall condition.

Observation: The flow symmetry in the downstream domain is being created by the wall condition in the first domain with no wall impact, as can be seen in Figure 10. The flow is asymmetric for other domains with a different boundary condition as a result of the impact of the wall condition.

Observation: From Figure 11, it can be seen that the wall effect in the upstream domain of the first domain with wall condition is absent. In contrast, the flow is asymmetric in other domains with a different boundary condition because of the influence of the wall condition.

Since the results from the first domain were quite practical and intuitive from the perspective of flow evolution, it was chosen as the best domain in comparison to the case where there is uncertainty on where to place pressure far field boundary conditions on the downstream domain. This is because the deviation was observed to be small and insignificant at various points in the downstream domain using wall boundary condition. As a result, the first domain with wall boundary requirements was chosen for more research.

To verify the sensitivity of the mesh against the projected outcomes, simulations were ran on the specified domain (First Domain) for three different grid sizes, with 6.8 million, 11.8 million, and 9.4 million elements, respectively. A grid independent study was completed by choosing the 6.8 million grid because it showed less deviation than the 11.8 million and 9.4 million grids. Analysis is conducted with the assumption that the flow is incompressible, steady state, and three dimensional (Table 3).

Observation: From Figure 12 it is observed that the 6.8 M grid showed up least deviation and lies in between 9.4 M and 11.8 M grid.

Observation: From Figure 13 it is observed that the 6.8 M grid showed up least deviation and lies in between 9.4 M and 11.8 M grid.

Observation: From Figure 14 it is observed that the 6.8 M grid showed up least deviation and lies in between 9.4 M and 11.8 M grid. The distribution of recirculation zone across different grids is shown in Figure 15.

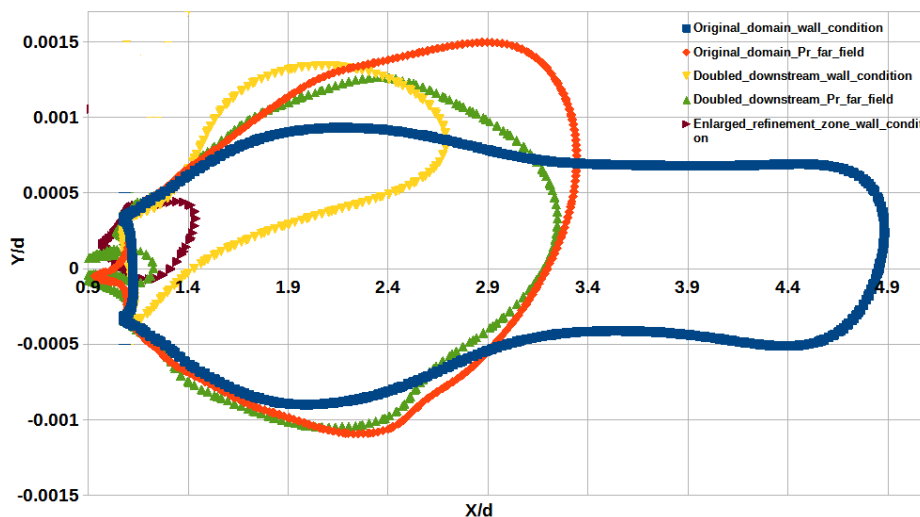


Figure 11. Distribution of re-circulation zone across different domain and B.C.

Table 3. The quality check for three grids

S.N.	Quality Check	6.8 Million	11.8 Million	9.4 Million
1.	Aspect ratio	25.5	26.2	27.4
2.	Orthogonality	0.1	0.1	0.1
3.	Skewness	0.8	0.8	0.8

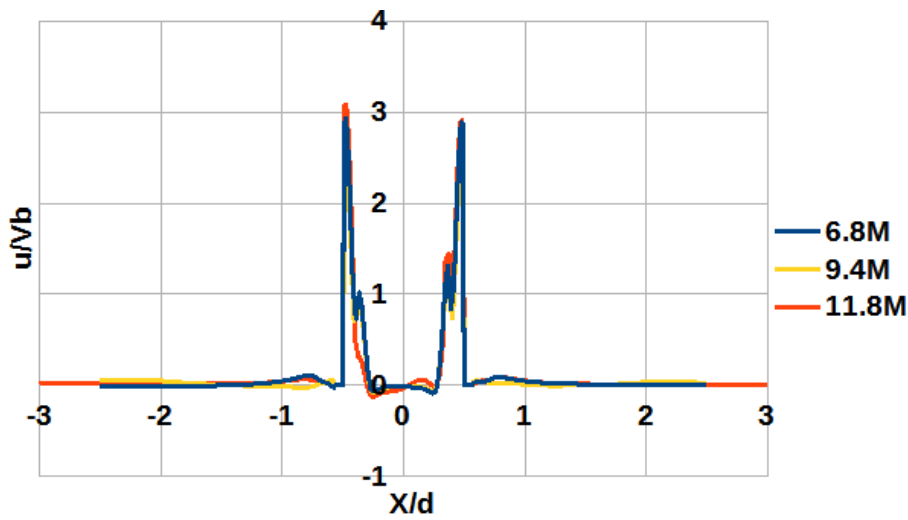


Figure 12. Distribution of axial velocity at $X/d=1.1$ across different grids.

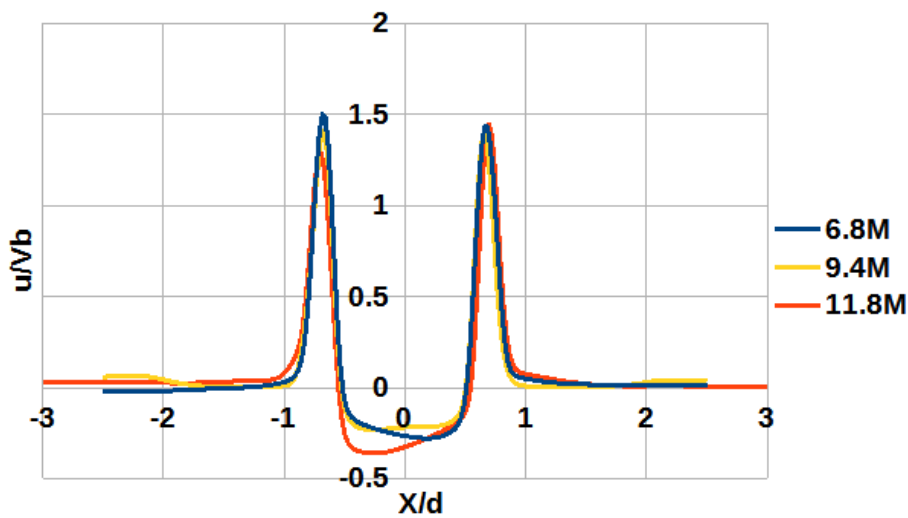


Figure 13. Distribution of axial velocity at $X/d=1.5$ across different grids.

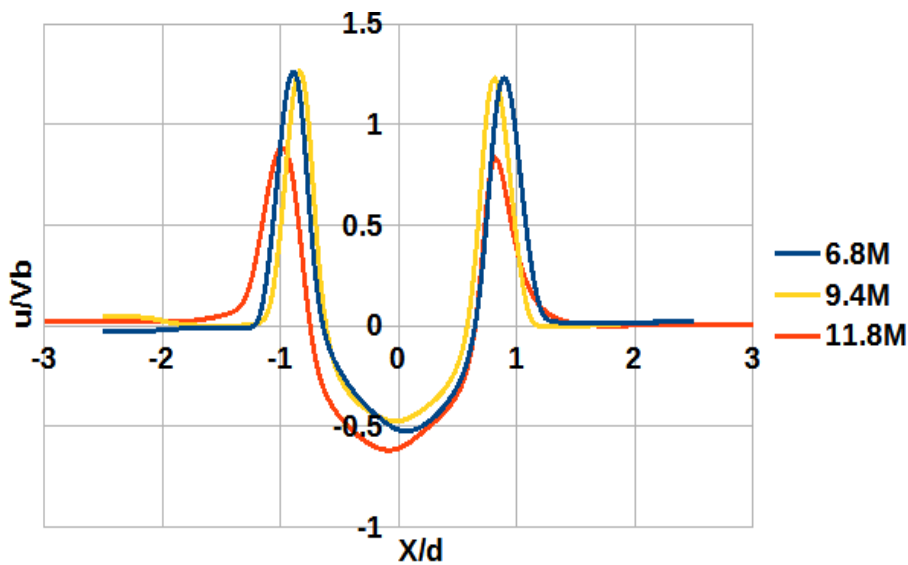


Figure 14. Distribution of axial velocity at $X/d=1.8$ across different grids.

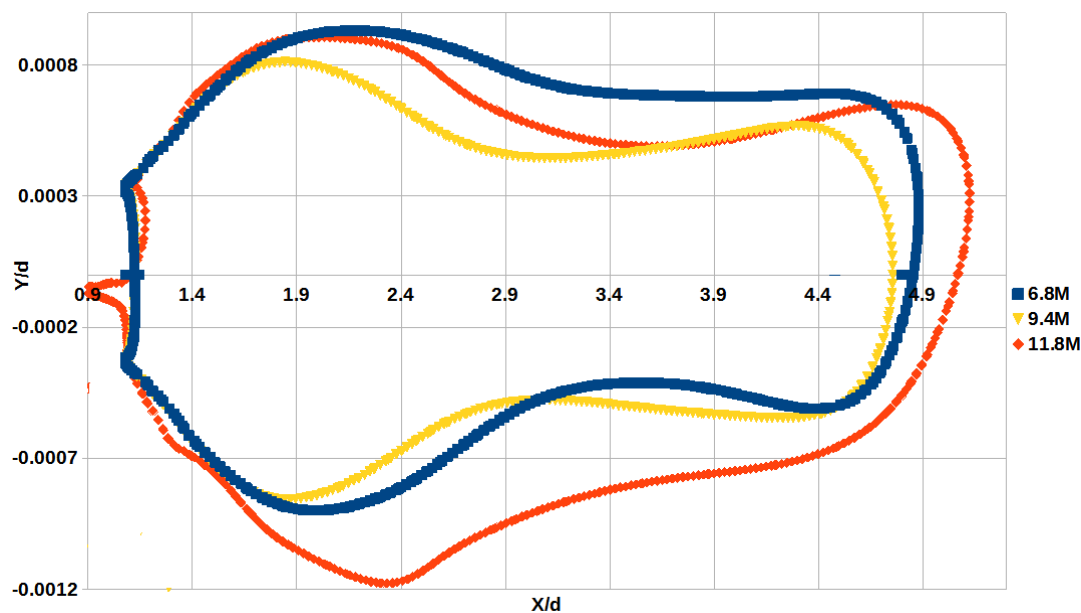


Figure 15. Distribution of re-circulation zone across different grids.

Solver Characteristic

Analysis was accomplished using ANSYS Fluent 19.5.0 is used. Rans primarily based analyses were accomplished considering the drift as consistent and incompressible. The k and ϵ values are solved one at a time by way of the usage of two specific independent equations for this reason referred to as the model as two equation model.

Turbulence Model

We used a specific mathematical model called the Realizable k - ϵ turbulence model to analyze the data. The model includes two equations and is commonly used when studying turbulence. The experiment was conducted using a specific method called a second-order upwind scheme.

Boundary Conditions

The mass flow rate and pressure at the inlet and outlet are assumed to be the same. The current computation takes into account the experimental setup's operating condition. The inlet and outlet temperatures are 303 K, the mass flow rate at the inlet is 0.04203 kg/s, and the pressure is atmospheric. The effect of relative motion between the jet surface and the surrounding air enhances the atomization process at higher velocities, whereas this analysis is done at atmospheric conditions.

RESULTS AND DISCUSSIONS

This section discusses the results of CFD analysis for grid selection and comparing the results for different mass flow rates with experimental results for validation.

Grid Selection

The figures. (12) axial velocity plot, (13) radial velocity plot, (14) tangential velocity plot and (15) re-circulation zone plot, shows the comparison of 6.8 million, 9.4 million and 11.8 million grid at three different location in the downstream domain was done and it was observed that the 6.8 million grid showed very less deviation at all the three location and was lying in between 9.4 million and 11.8 million grid. So the grid with 6.8 million was chosen as the best grid and the validation was continued.

Validation Study

The analysis was performed for the chosen first domain with 6.8 million grid by fixing the mass flow rate as 0.04203 kg/s, which was taken from experimental data.

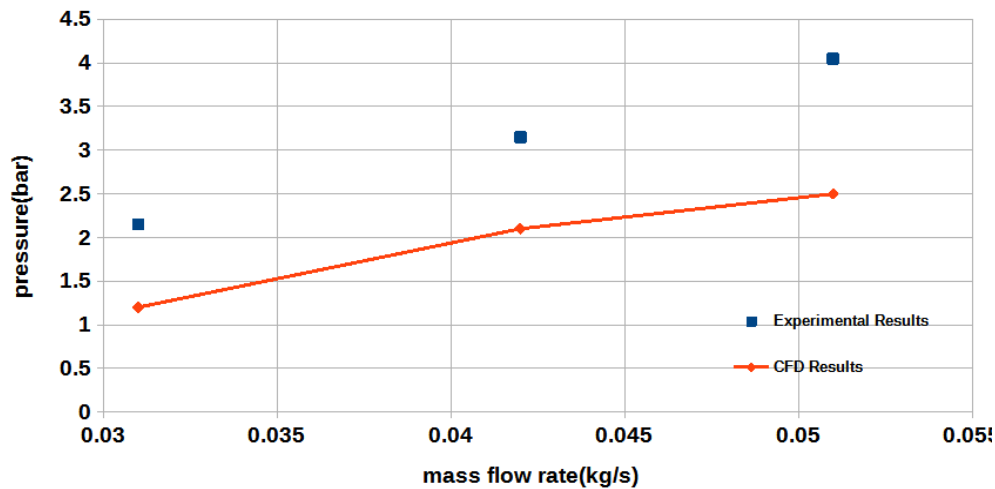


Figure 16. Comparison between experimental and CFD data with different mass flow rate (\dot{m} vs p plot).

Validations were also performed at two different mass flow rates 0.051 kg/s and 0.031 kg/s taken from experimental data and analyzed after the simulations for which a plots for \dot{m} vs p was plotted as shown below.

According to Figure 16, the trend for CFD results for which pressure was calculated followed the same trend as the experimental results. The pressure values, however, were discovered to be lower than the experimental pressures. This could be attributed to the consideration of measurement probe locations in the case of an experimental setup, as well as uncertainty in the current turbulence model's ability to capture pressure losses due to frictional effects using the type of grid resolutions.

CONCLUSIONS

RANS-based CFD study effectively captures the flow field of a flow inside the air blast injector, which is a crucial fundamental feature of flow physics. This study demonstrates the domain choice for the flow field study, optimal grid choice, and validation study by contrasting various experimental mass flow rates. The injector's egress from the injector lip is not far from the point of greatest axial velocity. This is because the existence of recirculated air bubbles, which limit the nozzle's exit, causes the local exit velocity of the nozzle to increase. The flow field of a flow inside an air blast injector, a vital fundamental aspect of flow physics, is efficiently captured by a RANS-based CFD analysis. By comparing various experimental mass flow rates, this study illustrates the domain selection for the flow field study, optimal grid selection, and validation investigation. The location of greatest axial velocity is not far from where the injector exits from the injector lip. This is due to the fact that the presence of recirculated air bubbles increases the nozzle's local exit velocity and limits its exit.

REFERENCES

1. Rayleigh, L., "On the Instability of Jets," Proceedings of London Mathematical Society, Vol. 10, pp. 4–13, 1878.
2. Lefebvre, A. H., Fuel effects on gas turbine combustion— Ignition, stability, and combustion efficiency, ASME J. Eng. Gas Turbines Power, Vol. 107, 1985, pp. 24–37.
3. Reeves, C. M., and Lefebvre, A. H., Fuel effects on aircraft combustor emissions, ASME Paper 86-GT-212,
4. Rink, K. K., and Lefebvre, A. H., Influence of fuel drop size and combustor operating conditions on pollutant emissions, SAE Technical Paper 861541, 1986
5. Atomization and Spray by Arthur H. Lefebvre and Vincent G. McDonell (Second edition).
6. Rampada Rana, Sonu Kumar and Nagalingam Muthuveerappan, "RANS Based Iso-Thermal CFD Analysis of the Flow Field Created by a Radial Swirler in a Conical Nozzle", GTINDIA2019-2726, <https://doi.org/10.1115/GTINDIA2019-2726>.

7. Hinze, J. O., "Fundamentals of the Hydrodynamic Mechanism of Splitting in Dispersion Processes," *AICHE Journal*, Vol. 1, No. 3, pp. 289–95, 1995.
8. Rampada Rana, Muthuveerappan Nagalingam and Saptarshi Basu, "Numerical Behaviour of Primary Air Flow Field of a Swirl Injector Under High Pressure and High Temperature Condition", *GTINDIA2021-76449*, <https://doi.org/10.1115/GTINDIA2021-76449>.
9. Rampada Rana, Muthuveerappan Nagalingam, "CFD Analysis Of Primary Air Flow Field Of A Swirl Injector Using Embedded LES Based Hybrid Model".
10. Sankaran, Vaidyanathan, Memon, Suresh, 2002, "LES of Spray Combustion in Swirling Flow", *Journal of Turbulence*, 3, N11, DOI: 10.1088/1468-5248/3/1/011.
11. Colket, M., Heyne, J., Rumizen, M., Gupta, M., Edwards, T., Roquemore, W. M., Andac, G., Boehm, R., Lovett, J., Williams, R., Condevaux, J., Turner, D., Rizk, N., Tishkoff, J., Li, C., Moder, J., Friend, D., and Sankaran, V., "Overview of the National Jet Fuels Combustion Program," *AIAA Journal*, Vol. 55, No. 4, 2017, pp. 1087–1104. doi:10.2514/1.J055361, URL <https://doi.org/10.2514/1.J055361>.
12. Chin, J. S., Rizk, N. K., and Razdan, M. K., "Study on Hybrid Airblast Atomization," *Journal of Propulsion and Power*, Vol. 15, No. 2, 1999, pp. 241–247. doi:10.2514/2.5418, URL <https://doi.org/10.2514/2.5418>.
13. Rizkalla, A. A., and Lefebvre, A. H., "The Influence of Air and Liquid Properties on Airblast Atomization," *ASME Journal of Fluids Engineering*, Vol. 97, No. 3, 1975, pp. 316–320. doi:10.1115/1.3447309, URL <http://fluidsengineering.asmedigitalcollection.asme.org/article.aspx?articleid=1422742>.
14. Rizkalla, A. A., and Lefebvre, A. H., "Influence of Liquid Properties on Airblast Atomizer Spray Characteristics," *ASME Journal of Engineering for Power*, Vol. 97, No. 2, 1975, pp. 173–177. doi:10.1115/1.3445951, URL <https://gasturbinespower.asmedigitalcollection.asme.org/article.aspx?articleID=1418766>.
15. Wang, X. F., and Lefebvre, A. H., "Influence of fuel temperature on atomization performance of pressure-swirl atomizers," *Journal of Propulsion and Power*, Vol. 4, No. 3, 1988, pp. 222–227. doi:10.2514/3.23052, URL <https://doi.org/10.2514/3.23052>.
16. Giffen, E., and Muraszew, A., *Atomization of Liquid Fuels*, Chapman and Hall, London, 1953.
17. Zheng, Q. P., Jasuja, A. K., and Lefebvre, A. H., "Influence of Air and Fuel Flows on Gas Turbine Sprays at High Pressures," *Twenty-Sixth Symposium (International) on Combustion*, pp. 2757–62, The Combustion Institute, Pittsburgh, PA, 1996.
18. Zheng, Q. P., Jasuja, A. K., and Lefebvre, A. H., "Structure of Airblast Sprays under High Ambient Pressure Conditions," *Journal of Engineering for Gas Turbines and Power*, Vol. 119, No. 3, pp. 512–18, 1997.
19. Chen, S. K., Lefebvre, A. H., and Rollbuhler, J., "Factors Influencing the Circumferential Liquid Distribution from Pressure-Swirl Atomizers," *Journal of Engineering for Gas Turbines and Power*, Vol. 115, pp. 447–52, 1993.
20. Rosfjord, T. J., and Eckerle, W. A., "Aerating Fuel Nozzle Design Influences on Airflow Features," *Journal of Propulsion and Power*, Vol. 7, No. 6, pp. 849–56, 1991.
21. Wang, H. Y., McDonell, V. G., and Samuelsen, G. S., "The Two-Phase Flow Downstream of a Production Engine Combustor Swirl Cup," *Twenty-Fourth Symposium (International) on Combustion*, pp. 1457–63, The Combustion Institute, Pittsburgh, PA, 1992.